Journal of Zhejiang University-SCIENCE C (Computers & Electronics)
ISSN 1869-1951 (Print); ISSN 1869-196X (Online)
www.zju.edu.cn/jzus; www.springerlink.com
E-mail: jzus@zju.edu.cn

A wavelet packet based method for adaptive single-pole auto-reclosing[#]

Sadegh JAMALI, Navid GHAFFARZADEH

(*Centre of Excellence in Power Systems Automation and Operation, Iran University of Science and Technology, Tehran, Iran*)

E-mail: sjamali@iust.ac.ir; ghaffarzadeh@ee.iust.ac.ir

Received Oct. 15, 2009; Revision accepted May 10, 2010; Crosschecked Sept. 28, 2010

Abstract: We present a new algorithm for adaptive single-pole auto-reclosing of power transmission lines using wavelet packet transform. The db8 wavelet packet decomposes the faulted phase voltage waveform to obtain the coefficients of the nodes 257, 259 to 262. An index is then defined from the sum of the energy coefficients of these nodes. By evaluating the index, transient and permanent faults, as well as the secondary arc extinction instant, can be identified. The significant advantage of the proposed algorithm is that it does not need a threshold level and therefore its performance is independent of fault location, line parameters, and operating conditions. Moreover, it can be used in transmission lines with reactor compensation. The proposed method has been successfully tested under a variety of fault conditions on a 400 kV overhead line of the Iranian National Grid using the Electro-Magnetic Transient Program (EMTP). The test results validated the algorithm's ability in distinguishing between transient arcing and permanent faults and determining the instant of secondary arc extinction.

Key words: Adaptive auto-reclosing, Arcing faults, Permanent faults, Transmission lines, Wavelet packet transform
doi:10.1631/jzus.C0910617 **Document code:** A **CLC number:** TM762.2

1 Introduction

Arcing accounts for most of the faults on overhead lines in transmission systems. More than 90% of arcing faults, which have a transient nature, are of the single-phase-to-earth type, where single-pole auto-reclosing (SPAR) can be applied to improve the system transient stability and hence the reliability. It has been shown in the literature that during single-phase faults half the pre-fault power can still be transferred by the healthy phases (Power System Relaying Committee Working Group, 1992; Ahn *et al*., 2001).

Most automatic reclosing techniques employ a prescribed reclosure time, thereby reclosing the breaker after a fixed dead time following a tripping operation. This method can pose problems in some cases. For example, when an arcing fault restrikes due to insufficient time for the fault path to fully deionize, fixed time auto-reclosing can cause adverse effects on the system stability and reliability. On the other hand, unsuccessful reclosing during a permanent fault may aggravate the potential damage to the system and equipment (Bo *et al*., 1997). For some extra-high-voltage lines, particularly those that are close to generating plants, fixed time auto-reclosing cannot be used and adaptive auto-reclosing schemes have therefore been introduced over the past decades (Bowler *et al*., 1980). These schemes prevent unsuccessful reclosing on permanent faults and during arcing faults, with reclosing accomplished only after full extinction of the secondary arc and complete deionization of the arc path.

Many methods have been proposed for the SPAR on transmission lines. Ge *et al*. (1989) used the voltage induced from healthy phases to the faulted one to recognize the fault condition. In Ahn *et al*. (2001), the root mean square (RMS) value of faulted phase voltage was calculated over a data window at each time step and then compared with the RMS value of

[#] A preliminary version was presented at the 24th International Power System Conference (PSC2009), Tehran, Iran

the previous time step. When the difference between the RMS values attained a value above a certain threshold level, a reclosing signal was generated. Bo *et al*. (1997) compared the power of high frequency current components of either of the healthy phases with a threshold level to discriminate the internal arcing fault condition from other conditions.

Lin *et al*. (2006) presented a dual-window transient energy ratio criterion based on a modal current. The authors showed that the energy ratio approaches unity under normal steady-state operation, whereas it increases greatly under fault conditions. Lin *et al*. (2007) further proposed a voltage based criterion called a dual-window transient energy ratio based on the faulted phase voltage.

Several researchers used artificial intelligence (AI) methodology in this area. Aggarwal *et al*. (1994), Fitton *et al*. (1996), and Yu and Song (1998) presented different adaptive auto-reclosing approaches based on artificial neural networks (ANNs). Aggarwal *et al*. (1994) used Fourier transform to extract various components of the faulted phase voltage and applied them to an ANN, which was trained by more than 25 000 permanent and transient single-phase-to-earth faults. Fitton *et al*. (1996) employed the short time Fourier transform (STFT) to extract proper feature vectors, which were the energy of voltage waveforms in five frequency bands and were applied in training the ANN. The network had five inputs, one hidden layer, and an output layer with one node. Hybrid schemes using ANN and wavelet transform (WT) were suggested by Yu and Song (1998), where the WT was used to extract feature vectors used as the ANN input to identify transient faults and the secondary arc extinction instant. Lin and Liu (1998) used the fuzzy logic concept to distinguish between permanent faults and transient faults.

Radojevic and Shin (2007) used the total harmonic distortion (THD) value of the faulted phase voltage to determine an appropriate time for reclosing. The fundamental component of the zero sequence power at both ends of a transmission line was used in Elkalashy *et al*. (2007) to detect the extinction time of the secondary arc. Jamali and Parham (2010) presented a new analytical method for the SPAR based on the zero sequence voltage.

This paper introduces a new algorithm for adaptive single-pole auto-reclosing, based on the wavelet packet transform (WPT), which can identify transient and permanent faults, as well as the secondary arc extinction instant.

2 Wavelet packet transform

WPT is a generalized version of the discrete wavelet transform, which gives a richer range of possibilities for signal analysis. In wavelet analysis, a signal is split into approximation and detail coefficients by passing it through low- and high-pass filters, respectively, in the first level of decomposition. The approximation is then split into a second-level approximation and detail, and the process is repeated. Therefore, the WPT decomposition forms a binary tree like structure as shown in Fig. 1 (Mallat, 1999).

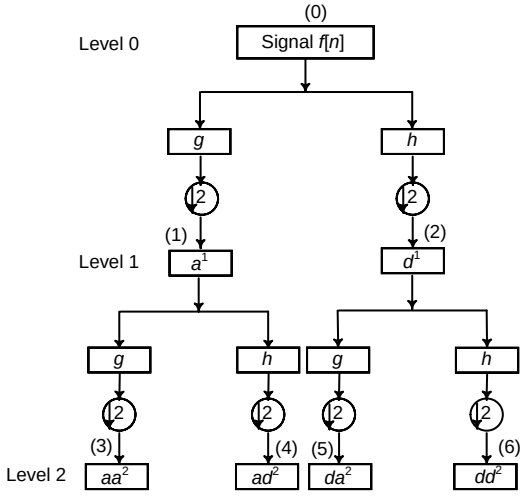

Fig. 1 Wavelet packet transform (WPT) decomposition of signal *f*[*n*]

In Fig. 1, blocks *g* and *h* are the low- and high-pass filters, respectively, which are determined by the mother wavelet. Coefficients of *g* and *h* are dependent on each other through the following relation (Zhuang and Baras, 1994; Saleh and Rahman, 2005; Misiti *et al*., 2007):

$$h_k = (-1)^k g_{L-K}, \quad k = 0,1,...,L-1. \tag{1}$$

Any filter bank that satisfies Eq. (1) is known as a quadrature mirror filter (QMF) bank (Pandey and Satish, 1998; Saleh and Rahman, 2005; Misiti *et al*., 2007). The first-level details $d^1[n]$ of a discrete signal

$f[n]$ are obtained as outputs of the high-pass filter (Chui, 1997; Misiti *et al*., 2007):

$$d^1[n]=\sum_{k=0}^{N-1}h(k)\,f(n-k). \tag{2}$$

The first-level approximations $a^1[n]$ for the same discrete signal $f[n]$ are outputs of the low-pass filter:

$$a^1[n]=\sum_{k=0}^{N-1}g(k)\,f(n-k). \tag{3}$$

Note that, in wavelet packet analysis, a^1 and d^1 are called nodes 1 and 2, respectively.

The translation is carried out through down-sampling by 2 after each filtering operation. The second-level details and approximation are determined by applying the same filters to a down-sampled one by 2 version of the discrete signal (Chui, 1997; Misiti *et al*., 2007):

$$aa^2[n]=\sum_{k=0}^{N/2-1}g(k)a^1(n-k), \tag{4}$$

$$ad^2[n]=\sum_{k=0}^{N/2-1}h(k)a^1(n-k), \tag{5}$$

$$da^2[n]=\sum_{k=0}^{N/2-1}g(k)d^1(n-k), \tag{6}$$

$$dd^2[n]=\sum_{k=0}^{N/2-1}h(k)d^1(n-k). \tag{7}$$

Note that, aa^2, ad^2, da^2, and dd^2 are called nodes 3, 4, 5, and 6, respectively. This procedure is repeated until the signal is decomposed to a certain pre-defined level, which depends on the frequency resolution.

3 System modeling

For the simulation purpose to validate the proposed algorithm, one of the important 400 kV transmission lines of the Iranian National Grid has been chosen. The 264 km line connects the Abbaspoor substation to the Araak substation. The system frequency is 50 Hz and the line has been modeled using the Marti model (Marti, 1982) based on the physical geometry of the line conductors shown in Fig. 2.

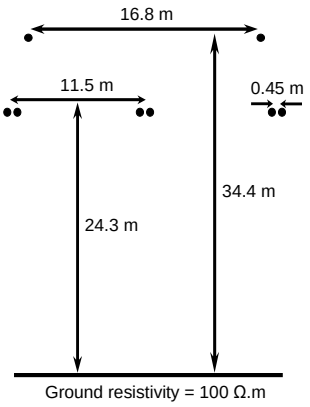

Fig. 2 Transmission-line conductor geometry

Fig. 3 shows the single-line diagram of the test system. The two-port model has been used for more accurate representation of the network. The zero and positive sequence impedances for this model are

$$Z_{1\text{Araak}}=1.7902+17.2186\text{i},$$
$$Z_{0\text{Araak}}=6.8554+20.3674\text{i},$$
$$Z_{1\text{Abbaspoor}}=0.6256+8.6006\text{i},$$
$$Z_{0\text{Abbaspoor}}=0.4511+5.3909\text{i},$$
$$Z_{1\text{Araak-Abbaspoor}}=6.6921+127.31\text{i},$$
$$Z_{0\text{Araak-Abbaspoor}}=259.24+654.84\text{i}.$$

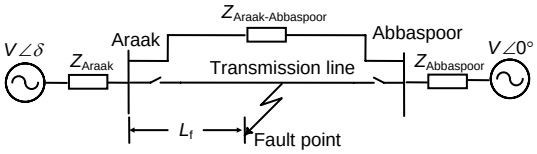

Fig. 3 Single-line diagram of the test system with a two-port model

Several arcing fault models have been proposed in the literature. Modeling techniques for arc phenomena have been improved by field experiments to simulate dynamic characteristics (Johns *et al*., 1994; Prikler *et al*., 2002). In this work, arcing faults have been modeled as presented in Johns *et al*. (1994). From a modeling point of view, arcing faults can be classified as high current primary arc during the fault and low current secondary arc after the faulted phase is isolated. The secondary arc is sustained by mutual coupling between the healthy and faulted phases (Johns *et al*., 1994).

An arcing earth fault on phase 'a' at 70 km from the Araak Bus has been simulated and the faulted phase voltage at this bus is illustrated in Fig. 4. It can be seen that following the fault occurrence at t_f=0.32 s, the bus voltage reduces. At t_b=0.37 s, the breaker interrupts the fault current and isolates the faulted phase. The time interval between t_b and t_q shows the behavior of the isolated phase voltage during the secondary arc period. At t_q=0.6417 s the secondary arc is quenched and the recovery voltage direct current (DC) offset appears due to the residual voltage of the transmission line.

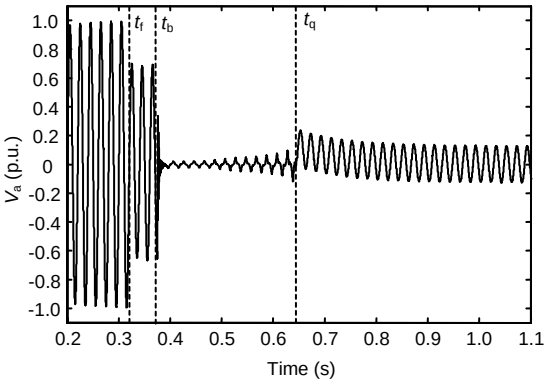

Fig. 4 Voltage waveform of the faulted phase 'a' for the single-phase-to-earth arcing fault

4 Selection of a proper wavelet packet

There are several wavelet packets, and a preprocessing procedure is required to select the most suitable one. The procedure is described here for the test system of Fig. 2. The criterion used to select the best wavelet packet is the average time delay index (ATDI) given by

$$\text{ATDI} = \frac{1}{N}\sum_{i=1}^{N}\Delta t_i, \tag{8}$$

where Δt_i is the difference between the reclosing command instant and the quenching instant for the ith case, and N is the number of simulated cases. Δt_i is calculated for N=8316 different cases as follows: (1) fault distance: 0 km$\le L_f \le$260 km at a step of Δl=10 km and L_f=264 km; (2) fault occurrence instant: 0.3 s$\le t_f \le$ 0.31 s at a step of Δt_f=0.001 s; (3) load angle: $-20° \le \delta \le 20°$ at a step of $\Delta\delta$=5°.

The above procedure is performed for three cases of uncompensated transmission line, transmission line with an isolated neutral shunt reactor, and transmission line with an earthed neutral shunt reactor.

ATDI has been calculated for 34 types of wavelet packets including: Haar, Daubechies (db2 to db10), Symlets (sym2 to sym9), Coiflets (coif1 to coif5), Biorthogonal (bior2.4, bior2.6, bior2.8, bior3.3, bior3.5, bior3.7, bior3.9, bior4.4, bior5.5, bior6.8), and discrete Meyer (dmey). The results are given in Table 1, where it can be seen that db8 has a better performance and offers a higher level of accuracy (minimum level of ATDI, 0.00501).

Table 1 Average time delay index (ATDI) of different types of wavelet packet

Wavelet packet	ATDI	Wavelet packet	ATDI
haar	0.01873	db4	0.00625
coif1	0.01742	db5	0.00836
coif2	0.01438	db6	0.00729
coif3	0.01509	db7	0.00763
coif4	0.01281	**db8**	**0.00501**
coif5	0.01165	db9	0.00705
dmey	0.02027	db10	0.00712
sym2	0.01242	bior2.4	0.01933
sym3	0.00998	bior2.6	0.01478
sym4	0.00816	bior2.8	0.01094
sym5	0.00980	bior3.3	0.01382
sym6	0.00924	bior3.5	0.01126
sym7	0.00951	bior3.7	0.00893
sym8	0.00709	bior3.9	0.00921
sym9	0.00892	bior4.4	0.00994
db2	0.01198	bior5.5	0.00965
db3	0.00854	bior6.8	0.00897

5 Algorithm

The new algorithm uses the faulted phase voltage signal, which is sampled at 20 kHz. Then, by using the db8 wavelet packet, the voltage signal is decomposed into scale 8 and the coefficients of node 257 (containing the frequency range 78.125–117.1875 Hz) and nodes 259 to 262 (containing the frequency range 156.25–312.5 Hz) are selected. Therefore, the index is defined as

$$\text{index} = \sum_{i=1}^{N}\sum_{k=257,\,k\neq 258}^{262} d_k(i)^2, \tag{9}$$

where d_k and N are the coefficients and the number of coefficients at node k, respectively.

Note that the index is evaluated after the line breakers have isolated the faulted phase from both ends. The index evaluation is delayed by one cycle to overcome transients produced during the opening period of the circuit breakers.

Fig. 5 shows that the behavior of the proposed index under arcing faults is completely different from that under permanent faults. In Fig. 5 a phase-a-to-earth fault occurs on the line at 0.331 s and the faulted phase is isolated at 0.381 s from both ends. The fault location is 130 km from the sending end of the line and the load angle is −10°.

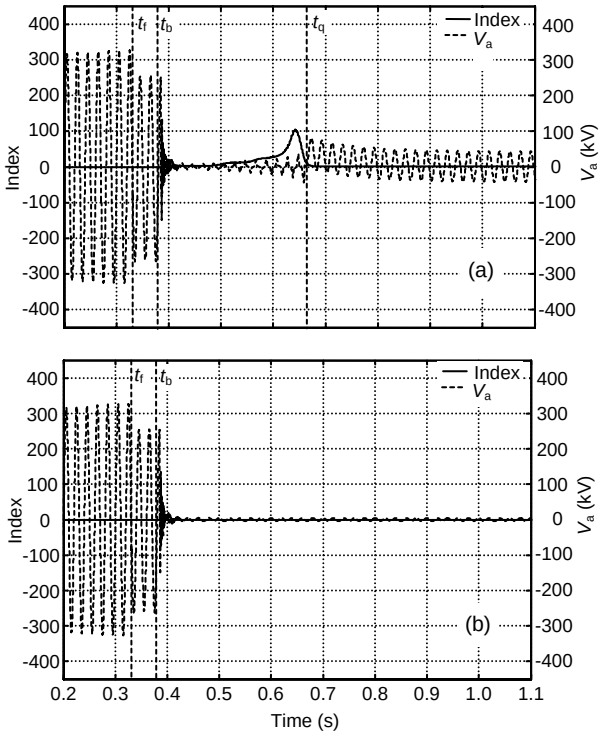

Fig. 5 Variation of the index during a transient fault (a) and a permanent fault (b)

Fig. 5a shows that after opening the breakers the index has a non-zero value for the transient fault (instant t_b), and once the secondary arc is quenched (instant t_q), it becomes zero. In contrast, Fig. 5b shows that during permanent faults, the index remains zero and does not change. This feature has been used to distinguish between permanent and transient faults and to determine the instant of secondary arc extinction. After opening the breakers, if the index remains null, the fault is permanent. Otherwise, the fault is transient and when the index becomes zero the secondary arc is quenched. The secondary arc extinction time is identified by evaluating the index.

In theory, to distinguish between permanent and transient faults and to determine the secondary arc extinction time, we need only to compare the index with zero. In practice, the index is compared with a small value, α, to overcome low amplitude variations of the index during permanent faults. In the test system, α is set to 0.75.

As mentioned before, the index is calculated after one cycle delay to overcome the transients produced during the opening period of the circuit breakers. The algorithm can be improved by disregarding this delay time and introducing an adaptive threshold level (ATL) after the breakers are opened. In order to calculate the ATL, the index value at each time step is added to its values at the previous time steps, and hence the ATL is formed as follows:

$$\mathrm{ATL}(k)=\frac{1}{f_s}\sum_{i=1}^{k}\mathrm{index}(i), \tag{10}$$

where f_s is the sampling rate. Actually, the ATL acts as a dynamic threshold level and therefore obviates the need for any fixed threshold level, which requires adjustment according to the transmission system. In other words, by using the ATL, the transient and permanent faults as well as the secondary arc extinction instant can be identified for different transmission systems without any threshold level adjustment.

6 Simulation study

Numerous simulation tests have been run to investigate the validity of the proposed algorithm under different fault conditions on the transmission lines with/without reactor compensation. The fault conditions include different load angles, fault occurrence instants, and fault locations. For brevity, only the selected test results are presented.

6.1 Line without reactor compensation

Three cases are considered for the line without reactor compensation. For all the cases the fault is a single-phase-to-earth one involving phase ‘a’.

In the first case, it is assumed that the fault occurs at 0.32 s and at 10 km from the Araak Bus. The load angle is 15° and the breakers open at 0.37 s. Fig. 6a shows the algorithm performance under

this fault condition. Fig. 6b depicts the algorithm performance under a permanent fault for the same conditions.

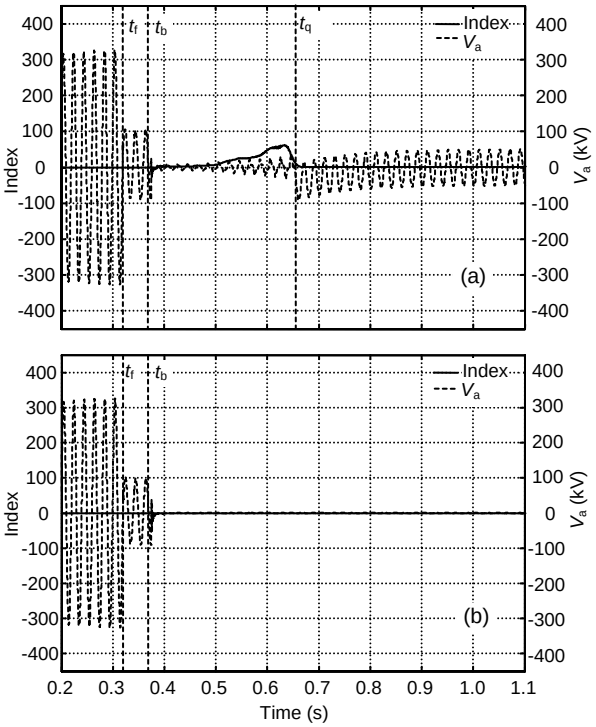

Fig. 6 Algorithm performance on the uncompensated line for a transient fault (a) and a permanent fault (b)
The fault occurs at 0.32 s and at 10 km from the Araak Bus. The load angle is 15° and the breakers open at 0.37 s

As shown in Fig. 6a, during an arcing fault and after the breakers opening, the index has a non-zero value and as the secondary arc quenches, the index becomes zero, whereas in Fig. 6b the index remains zero and does not change during a permanent fault.

In the second case, it is assumed that the fault occurs at 0.334 s and at 230 km from the sending end bus. Both the line end breakers isolate the faulted phase at 0.384 s and for the load angle of 5°. Figs. 7a and 7b show the algorithm performance for the transient and permanent faults, respectively.

In the third case, the fault occurs at 0.328 s and at the distance of 155 km from the Araak Bus. The load angle is −5° and the breakers open at 0.378 s. Figs. 8a and 8b show the algorithm performance under transient and permanent faults, respectively.

Fig. 9 provides more test results for different load angles and fault locations. It is assumed that the fault occurs at 0.33 s and the faulted phase is isolated at 0.38 s by opening both line end breakers.

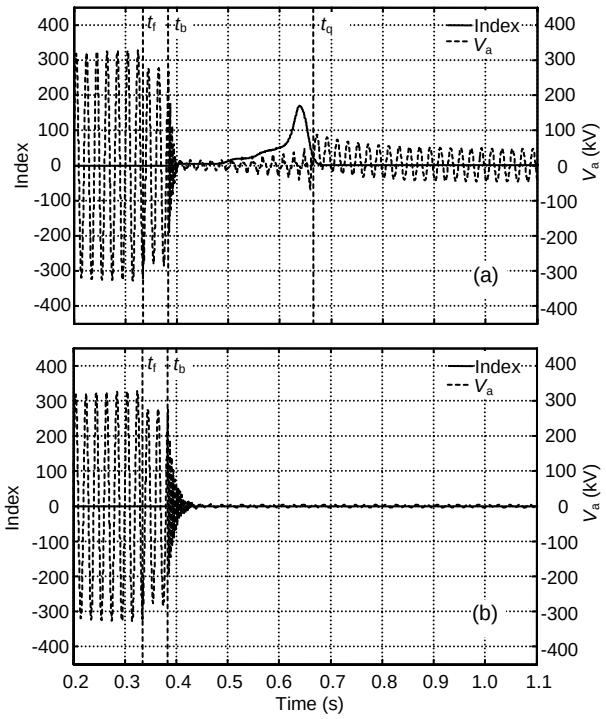

Fig. 7 Algorithm performance on the uncompensated line for a transient fault (a) and a permanent fault (b)
The fault occurs at 0.334 s and at 230 km from the sending end bus. Both the line end breakers isolate the faulted phase at 0.384 s and for the load angle of 5°

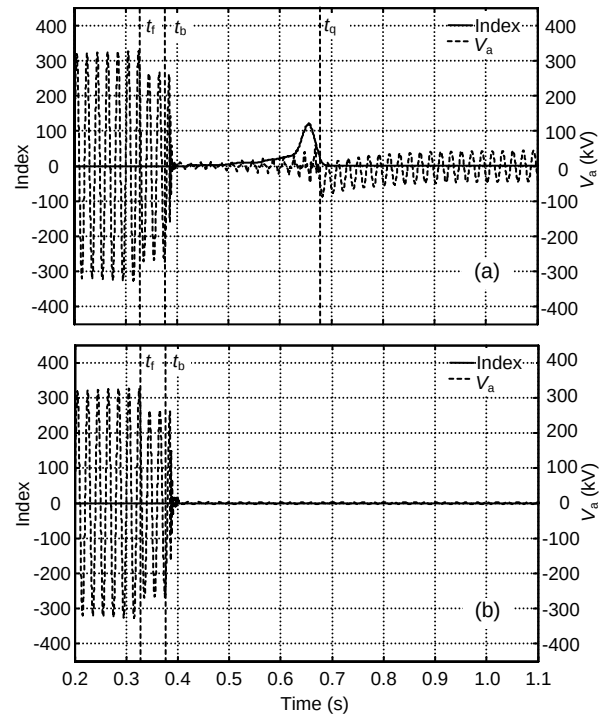

Fig. 8 Algorithm performance on the uncompensated line for a transient fault (a) and a permanent fault (b)
The fault occurs at 0.328 s and at the distance of 155 km from the Araak Bus. The load angle is −5° and the breakers open at 0.378 s

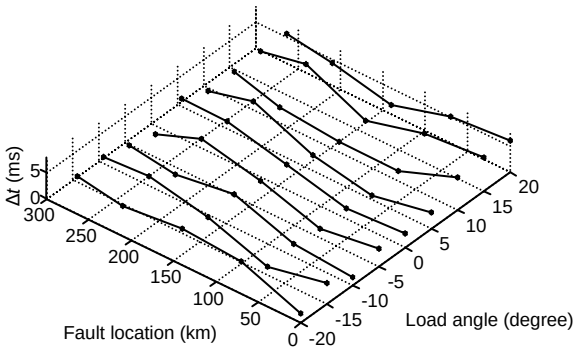

Fig. 9 Test results for different fault conditions

Δt is the difference between the secondary arc quenching instant and the reclosing command instant

Figs. 6–9 show the correct performances of the algorithm for different load angles, fault locations, and fault occurrence instants.

6.2 Line with reactor compensation

According to the analysis presented in Li *et al*. (2004) for transmission lines with a shunt reactor, the residual voltage of isolated phase consists of the residual voltage coupled from both the sound phases and the free oscillation frequency component due to electromagnetic induction by the line capacitance and the compensation reactors. Therefore, the compound residual voltage on the isolated phase will appear as a swing behavior, which does not permit most previous automatic reclosing techniques to be directly applied to transmission lines with reactor compensation.

Our proposed algorithm is immune to the swing behavior. This is shown by simulation tests performed for the case where a three-phase 50 MVar reactor is connected at each end of the line. Each 50 MVar reactor has been modeled by a 40 Ω resistance in series with a 5000 Ω reactance. The results for both permanent and arcing faults involving phase-a-to-earth are given for the three cases.

In the first case, it is assumed that the 50 MVar shunt reactors are with earthed neutral and that the fault occurs at 0.323 s and at a distance of 145 km from the sending end bus. The line end breakers isolate the faulted phase at 0.373 s and the load angle is 0°.

Figs. 10a and 10b show the correct algorithm performance under transient and permanent faults, respectively, under the same condition.

In the second case, it is assumed that the 50 MVar shunt reactors are with isolated neutrals and that the fault occurs at 0.332 s and at a distance of 240 km from the Araak Bus. The load angle is −5° and the breakers open the line at 0.382 s. Fig. 11a illustrates the algorithm performance for the transient fault, whereas Fig. 11b depicts the performance for the permanent fault.

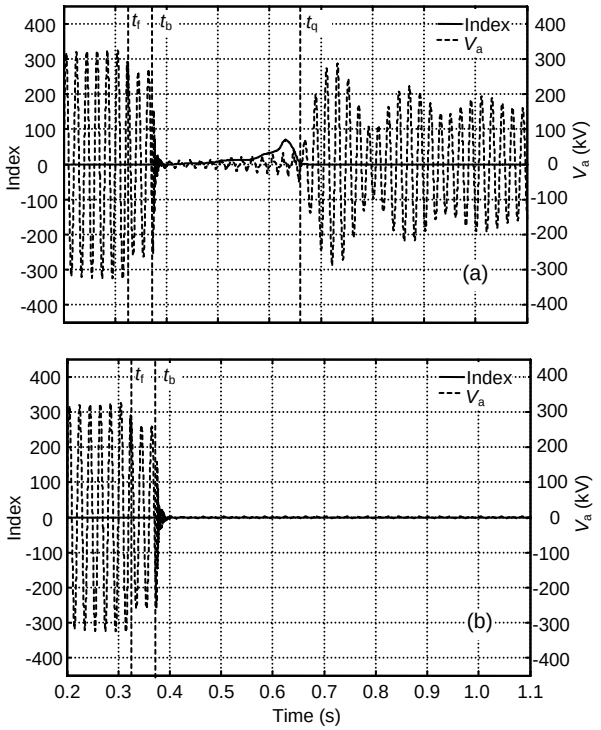

Fig. 10 Algorithm performance on transmission line with an earthed neutral shunt reactor for an arcing fault (a) and a permanent fault (b)

Fig. 12a shows more results for the line with an earthed neutral shunt reactor for various load angles and fault locations. Similarly, Fig. 12b shows the results for the line with an isolated neutral shunt reactor. It is assumed that the fault occurs at 0.32 s and the breakers open at 0.37 s.

To reduce the secondary arc duration for reactor compensated lines, one method is to use a single-phase reactor in the neutral of the shunt reactor. To justify this method, it is assumed that a 50 MVar shunt reactor with a 927 Ω neutral reactor is installed at both line ends. The appropriate amount of neutral reactor (927 Ω) is determined based on the analysis given in Power System Relaying Committee Working Group (1992). It is assumed that a phase-a-to-earth fault occurs at 0.338 s and at 90 km from the Araak Bus. The load angle is −10° and the breakers open at 0.388 s.

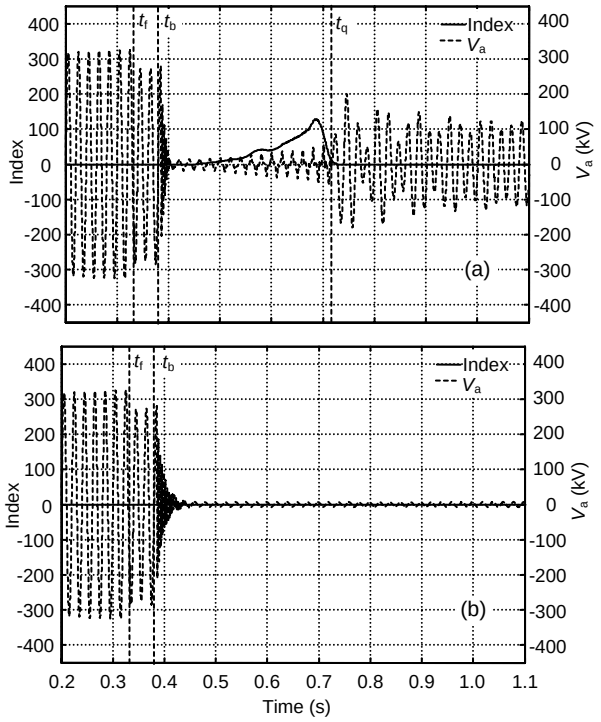

Fig. 11 Algorithm performance on transmission line with an isolated neutral shunt reactor for an arcing fault (a) and a permanent fault (b)

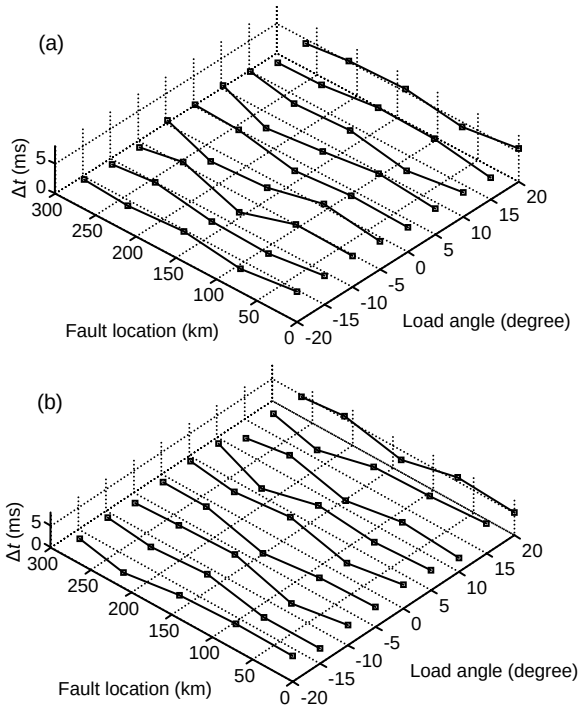

Fig. 12 Test results for the transmission line with an earthed neutral shunt reactor (a) and an isolated neutral shunt reactor (b) under different fault conditions

Δt is the difference between the secondary arc quenching instant and the reclosing command instant

Figs. 13a and 13b show the algorithm performance for the transient and permanent faults, respectively.

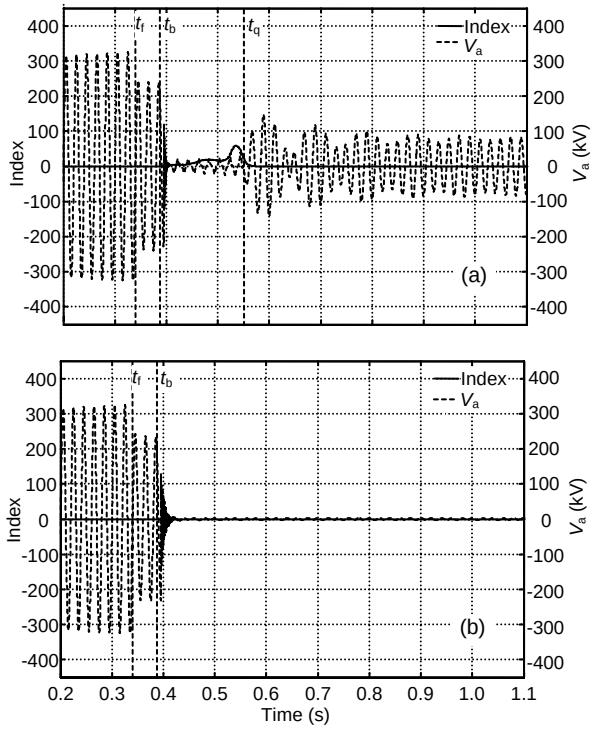

Fig. 13 Algorithm performance on transmission line with shunt compensation and with a neutral reactor for an arcing fault (a) and a permanent fault (b)

Figs. 10–13 show that the algorithm can correctly discriminate between transient and permanent faults and determine the secondary arc extinction instant for the shunt reactor compensated transmission lines. This is a significant advantage of the proposed method over previous methods.

7 Conclusions

A new algorithm for adaptive single-pole autoreclosing has been proposed using wavelet packet transfer (WPT). In this algorithm, the faulted phase voltage is captured with a sampling rate of 20 kHz. Then the db8 wavelet packet is used to decompose the signal to level 8 and to define an index, which is obtained from the sum of the coefficients energy of nodes 257 and 259 to 262. Finally, by evaluating the index value, the transient and permanent faults as well as the secondary arc extinction instant can be

identified. The proposed algorithm does not require an AI tool like ANN, nor does it need case based threshold level; hence, its results are independent of the system operation and fault conditions. The algorithm can also be used in transmission lines with reactor compensation. The accuracy and sensitivity of the algorithm have been verified by simulation studies under different fault conditions.

References

Aggarwal, R.K., Johns, A.T., Song, Y.H., Dunn, R.W., Fitton, D.S., 1994. Neural-network based adaptive single-pole autoreclosure technique for EHV transmission systems. *IEE Proc.-Gener. Transm. Distr.*, **141**(2):155-160. [doi:10.1049/ip-gtd:19949864]

Ahn, S.P., Kim, C.H., Aggarwal, R.K., Johns, A.T., 2001. An alternative approach to adaptive single pole autoreclosing in high voltage transmission systems based on variable dead time control. *IEEE Trans. Power Del.*, **16**(4):676-686. [doi:10.1109/61.956756]

Bo, Z.Q., Aggarwal, R.K., Johns, A.T., 1997. A Novel Technique to Distinguish Between Transient and Permanent Fault Based on Detection of Current Transients. Proc. 4th Int. Conf. on Advances in Power System Control and Management, p.216-220. [doi:10.1049/cp:19971833]

Bowler, C.E.J., Brown, P.G., Walker, D.N., 1980. Evaluation of the effect of power circuit breaker reclosing practices on turbine-generator shafts. *IEEE Trans. Power Appar. Syst.*, **99**(5):1764-1779. [doi:10.1109/TPAS.1980.319766]

Chui, C.K., 1997. Wavelets: a Mathematical Tool for Signal Processing. SIAM, Philadelphia, PA.

Elkalashy, N.I., Darwish, H.A., Taalab, A.M.I., Izzularab, M.A., 2007. An adaptive single pole autoreclosure based on zero sequence power. *Electr. Power Syst. Res.*, **77**(5-6):438-446. [doi:10.1016/j.epsr.2006.04.006]

Fitton, D.S., Dunn, R.W., Aggarwal, R.K., Johns, A.T., Bennett, A., 1996. Design and implementation of an adapative single pole autoreclosure technique for transmission lines using artificial neural networks. *IEEE Trans. Power Del.*, **11**(2):748-755. [doi:10.1109/61.489331]

Ge, Y., Sui, F., Xiao, Y., 1989. Prediction methods for preventing single-phase reclosing on permanent fault. *IEEE Trans. Power Del.*, **4**(1):114-121. [doi:10.1109/61.19197]

Jamali, S., Parham, A., 2010. New approach to adaptive single pole auto-reclosing of power transmission lines. *IET Gener. Transm. Distr.*, **4**(1):115-122. [doi:10.1049/iet-gtd.2009.0058]

Johns, A.T., Aggarwal, R.K., Song, Y., 1994. Improved technique for modelling fault arcs on faulted EHV transmission systems. *IEE Proc.-Gener. Transm. Distr.*, **141**(2):148-154. [doi:10.1049/ip-gtd:19949869]

Li, B., Li, Y.L., Sheng, K., Zeng, Z.A., 2004. The study on single-pole adaptive reclosure of EHV transmission lines with the shunt reactor. *Proc. CSEE*, **24**(5):52-56.

Lin, X., Liu, P., 1998. Method of Distinguishing Between Instant and Permanent Faults of Transmission Lines Based on Fuzzy Decision. IEEE Int. Conf. on Energy Management and Power Delivery, **2**:445-460. [doi:10.1109/EMPD.1998.702702]

Lin, X., Liu, H., Weng, H., Lu, W., Liu, P., Bo, Z.Q., 2006. A novel adaptive single-phase reclosure scheme using dual-window transient energy ratio and mathematical morphology. *IEEE Trans. Power Del.*, **21**(4):1871-1877. [doi:10.1109/TPWRD.2006.881427]

Lin, X., Liu, H., Weng, H., Liu, P., Wang, B., Bo, Z.Q., 2007. A dual-window transient energy ratio-based adaptive single-phase reclosure criterion for EHV transmission line. *IEEE Trans. Power Del.*, **22**(4):2080-2086. [doi:10.1109/TPWRD.2007.905346]

Mallat, S.G., 1999. A Wavelet Tour of Signal Processing (2nd Ed.). Academic Press, San Diego, CA.

Marti, J.R., 1982. Accurate modeling of frequency-dependent transmission lines in electromagnetic transient simulations. *IEEE Trans. Power Appar. Syst.*, **101**(1):147-155. [doi:10.1109/TPAS.1982.317332]

Misiti, M., Misiti, Y., Oppenheim, G., Poggi, J.M., 2007. Wavelet Toolbox 4 User's Guide. MathWorks Inc.

Pandey, S.K., Satish, L., 1998. Multiresolution signal decomposition: a new tool for fault detection in power transformers during impulse tests. *IEEE Trans. Power Del.*, **13**(4):1194-1200. [doi:10.1109/61.714484]

Power System Relaying Committee Working Group, 1992. Single phase tripping and auto reclosing of transmission lines IEEE committee report. *IEEE Trans. Power Del.*, **7**(1):182-192. [doi:10.1109/61.108906]

Prikler, L., Kizilcay, M., Ban, G., Handl, P., 2002. Improved Secondary Arc Models Based on Identification of Arc Parameters from Staged Fault Test Records. Proc. 14th Power Systems Computation Conf., p.1-7.

Radojevic, Z.M., Shin, J.R., 2007. New digital algorithm for adaptive reclosing based on the calculation of the faulted phase voltage total harmonic distortion factor. *IEEE Trans. Power Del.*, **22**(1):37-41. [doi:10.1109/TPWRD.2006.886781]

Saleh, S.A., Rahman, M.A., 2005. Modeling and protection of a three-phase power transformer using wavelet packet transform. *IEEE Trans. Power Del.*, **20**(2):1273-1282. [doi:10.1109/TPWRD.2004.834891]

Yu, I.K., Song, Y.H., 1998. Wavelet transform and neural network approach to developing adaptive single-pole auto-reclosing schemes for EHV transmission systems. *IEEE Power Eng. Rev.*, **18**(11):62-64. [doi:10.1109/39.726911]

Zhuang, Y., Baras, J.S., 1994. Optimal wavelet basis selection for signal representation. *SPIE*, **2242**:200-211. [doi:10.1117/12.170025]